Peer-Reviewed Technical Communication

Influence of Sea State and Tidal Height on Wave Power Absorption

Valeria Castellucci, Jessica García-Terán, Mikael Eriksson, Laurence Padman, and Rafael Waters

***Abstract*—The wave energy converter developed at Uppsala University (Uppsala, Sweden) consists of a linear generator placed on the seabed and driven by the motion of a buoy on the water surface. The buoy is connected to the moving part of the linear generator, the translator, which is made of ferrite magnets. The translator moves vertically inducing voltage in the windings of a fixed component, the so-called stator. The energy conversion of the linear generator is affected by the sea state and by variations of mean sea level. The sea state influences the speed and the stroke length of the translator, while the variation of tidal level shifts the average position of the translator with respect to the center of the stator. The aim of this study is to evaluate the energy absorption of the wave energy converter at different locations around the world. This goal is achieved by developing a hydromechanic model which analyses the optimum generator damping factor for different wave climates and the power absorbed by the generator, given a fixed geometry of the buoy and a fixed stroke length of the translator. Economic considerations regarding the optimization of the damping factor are included within the paper. The results suggest a nominal damping factor and show the power absorption losses at various locations, each of them characterized by a different wave climate and tidal range. The power losses reach up to 67% and in many locations a tidal compensation system, included in the design of the wave energy converter, is strongly motivated.**

I. Introduction

THE Uppsala University (Uppsala, Sweden) wave energy converter (WEC) consists of a linear generator at the seabed driven by the motion of a buoy on the surface; see Fig. 1. The translator moves vertically inside the stator and induces voltage in its windings [1].

The energy conversion of the linear generator depends on the sea state at the deployment site and on variations of the mean sea level. The sea state influences the speed and the stroke length of the translator [2]–[4], while the variation of the tidal level shifts the average position of the translator with respect to the center of the stator [5], [6].

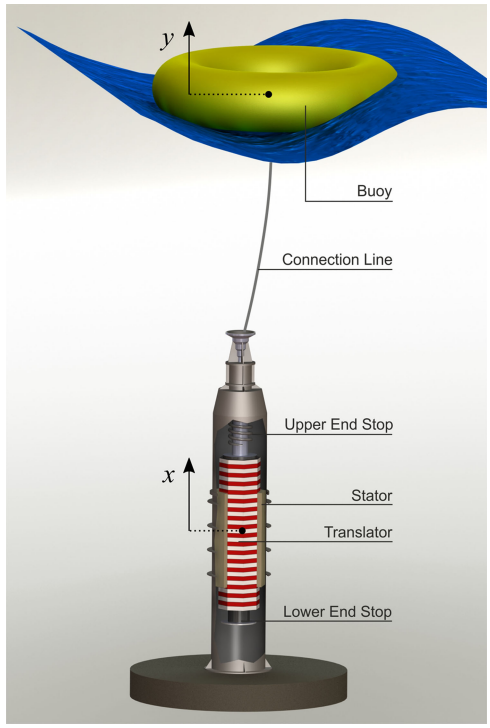

Fig. 1. Illustration of the wave energy converter (courtesy of Erik Lejerskog).

Experiments have demonstrated that the motion of the translator in linear generators is affected not only by the sea state, but also by the damping coefficient γ [4]. In fact, the translator speed $\dot{x}$ and the power absorption P will be affected by the generator electric behavior [7], which can be described by the damping force defined as $F_d = \gamma\dot{x}$. This force will influence the hydromechanic model presented in Section II-A.

The first aim of this study is to calculate the value of the damping coefficient that maximizes the power absorption of the WEC for different dominating sea states. Linear damping, i.e., a constant damping coefficient, is studied. Once the damping coefficient is optimized, the power losses of the generator due to the tidal effect can be evaluated at different coastal sites around the world. Today, the damping factor is affected by the wave climate and the generator design. However, control systems to regulate the damping in the WEC in real time could be developed in the near future.

Manuscript received January 27, 2016; revised April 26, 2016 and June 10, 2016; accepted August 1, 2016. Date of publication September 8, 2016; date of current version July 12, 2017. This work was supported by the Swedish Energy Agency, the ÅForsk Foundation, and the Carl Tryggers Foundation.

Associate Editor: M. Atmanand.

V. Castellucci, M. Eriksson and R. Waters are with the Division of Electricity, Department of Engineering Sciences, Uppsala University, Uppsala SE-751 21, Sweden (e-mail: valeria.castellucci@Angstrom.uu.se; mikael.eriksson@angstrom.uu.se; rafael.waters@angstrom.uu.se).

J. García Teráan is with the Industrial Engineering & Management, Department of Engineering Sciences, Uppsala University, Uppsala SE-751 21 Sweden (e-mail: jessica.garcia@angstrom.uu.se).

L. Padman is with the Earth & Space Research, Corvallis, OR 97333-1536 USA (e-mail: padman@esr.org).

Digital Object Identifier 10.1109/JOE.2016.2598480

Section II-B proposes an economic approach to the problem of damping optimization; its goal is to estimate the viable investment cost for a generator upgrade. In fact, the design of the generator needs to be adapted to the wave climate which characterizes different geographical sites, independently from the tidal effect.

II. Method

A. WEC Model

The model developed in this study couples the buoy hydrodynamic equation of motion (1) with the generator electromechanical equation (2)

$$m_b\ddot{y} = F_e - F_r + F_h - F_{gb} + F_b - F_w \tag{1}$$

$$m_t\ddot{x} = F_w - F_d - F_{gt} + F_{es} \tag{2}$$

where m_b and m_t are the buoy and the translator masses, $\ddot{y}$ and $\ddot{x}$ are the buoy and translator accelerations, F_e and F_r are the excitation and radiation forces, F_h is the restoring force, F_{gb} and F_{gt} are the gravity forces due to the buoy and translator masses, respectively, F_b is the buoyancy force, F_w is the connection line force between the buoy and the translator, F_d is the damping force, and F_{es} is the end-stop force. These two second-order differential equations are thoroughly described in many articles, e.g., in [7] and [8]. However, a brief definition of the forces is given below. In time domain, the hydrodynamic forces F_e and F_r can be expressed, respectively, as

$$F_e(t) = f_e(t) * \eta(t) \tag{3}$$

$$F_r(t) = m_a^{\infty}\ddot{y} + L(t) * \dot{y}(t) \tag{4}$$

where f_e is the transfer function which describes the relation between the excitation force and the incident wave η, m_a^{∞} is the added mass at the infinite frequency limit, and L is the impulse response function. L, f_e, and m_a are calculated by a wave interaction analysis tool (WAMIT) on the basis of the buoy shape and draft. Finally, the operator $*$ denotes the convolution between two functions. The restoring force is calculated as

$$F_h = -\rho g \pi r^2 y \tag{5}$$

where r is the radius and y is the displacement of the cylindrical buoy.

The connection line is modeled as damped single harmonic oscillator

$$F_w = \begin{cases} k_w(y-x) + d_w(\dot{y}-\dot{x}), & \text{if } y > x \\ 0, & \text{otherwise} \end{cases} \tag{6}$$

where k_w is the spring constant and d_w is the damping coefficient of the wire.

The end-stop force is the sum of the contribution of the upper end stop f_u, the lower end stop f_l, and the upper wall of the WEC capsule f_c. The force exerted by the hull of the WEC f_c is modeled as a stiff damped single harmonic oscillator, which the translator hits when the stresses on the upper end-stop spring start to provoke irreversible deformations, i.e., once the upper end stop is compressed by the length l_i. The following equations describe each contribution to the end-stop force:

$$f_u = \begin{cases} -k_e(x - l_s/2), & \text{if } x > l_s/2 \\ 0, & \text{otherwise} \end{cases} \tag{7}$$

$$f_l = \begin{cases} -k_e(x + l_s/2), & \text{if } x < -l_s/2 \\ 0, & \text{otherwise} \end{cases} \tag{8}$$

$$f_c = \begin{cases} -k_c(x - (l_s/2 + l_i)) + d_c\dot{x}, & \text{if } x \geq l_s/2 + l_i \\ 0, & \text{otherwise.} \end{cases} \tag{9}$$

The upper and lower end stops are springs having the same spring constant k_e, while k_c is a fictitious constant for the wall, as well as the damping factor d_c. The stroke length of the translator is l_s, and the middle point of the translator when centered with respect to the stator is found at $x = 0$.

The damping force F_d, defined in Section I, leads to the calculation of the generator power output $P = F_d\dot{x}$.

To simulate the WEC behavior, it is necessary to feed the model with a wave input: the two-parameter Bretschneider spectrum is chosen to generate random waves [9]. The chosen parameters of the spectrum S(ω) are a combination of significant wave height H_s and energy period T_e

$$S(\omega) = \frac{5\,\omega_m^4}{16\,\omega^5} H_s^2 e^{-5\omega_m^4/4\omega^4} \tag{10}$$

where ω is the frequency in radians per second, and ω_m is the modal (most likely) frequency of any given wave, which is a function of T_e.

From the Bretschneider spectrum, time series of the polychromatic waves are created. These are then superimposed onto a harmonic wave with a much longer period and an amplitude $a_t = H_t/2$, where H_t is the height of the tide at a chosen location. The simulations are carried out in 407 coastal points around the world, each one of them characterized by a combination of H_s, T_e, and H_t.

The data source for the first two parameters is The European Centre For Medium-Range Weather Forecast (ECMWF), which produces the global atmospheric reanalysis data set, ERA-Interim. ECMWF uses its forecast models and data assimilation systems to reanalyse the observations, from 1979 to present, with a temporal resolution of 6 h [10], [11]. The significant wave height and energy period used in the study presented here are averages calculated over ten years of modeled data. Fig. 2 shows the average H_s around the world and points out in which coastal areas the highest wave power potential is located, the available ocean power being proportional to the square of the wave height [12].

The third parameter H_t is obtained by estimating a time series of the tidal range in 28-h overlapping windows, then averaging over one year. The 28-h window captures the range for the variety of tides from purely semidiurnal to diurnal. The data set of tidal range was generated from the TPXO7.2 global inverse tide model [13], using the tidal model driver (TMD) Matlab toolbox developed by Earth & Space Research and Oregon State University. The H_t values in coastal areas around the world are presented in Fig. 3.

The input parameters which characterize the L12 generator are, among others, the stroke length of the translator (approxi-

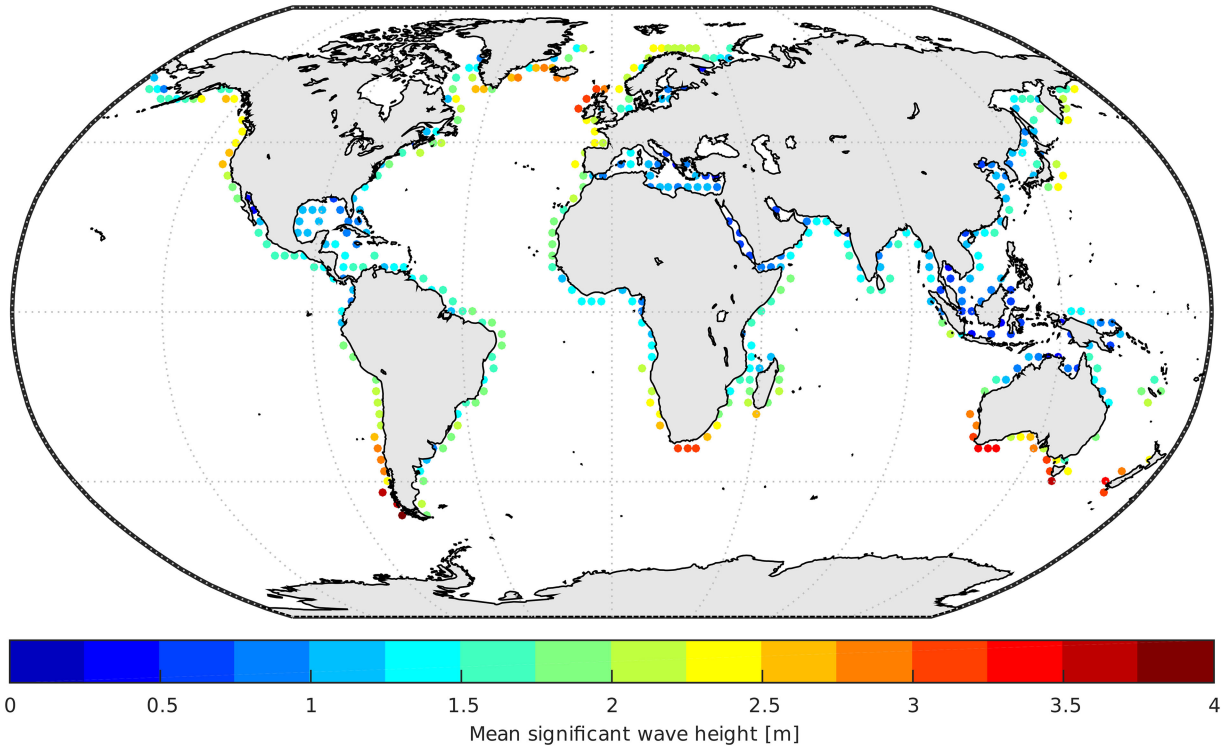

Fig. 2. Mean significant wave height calculated over ten years of ECMWF modeled data.

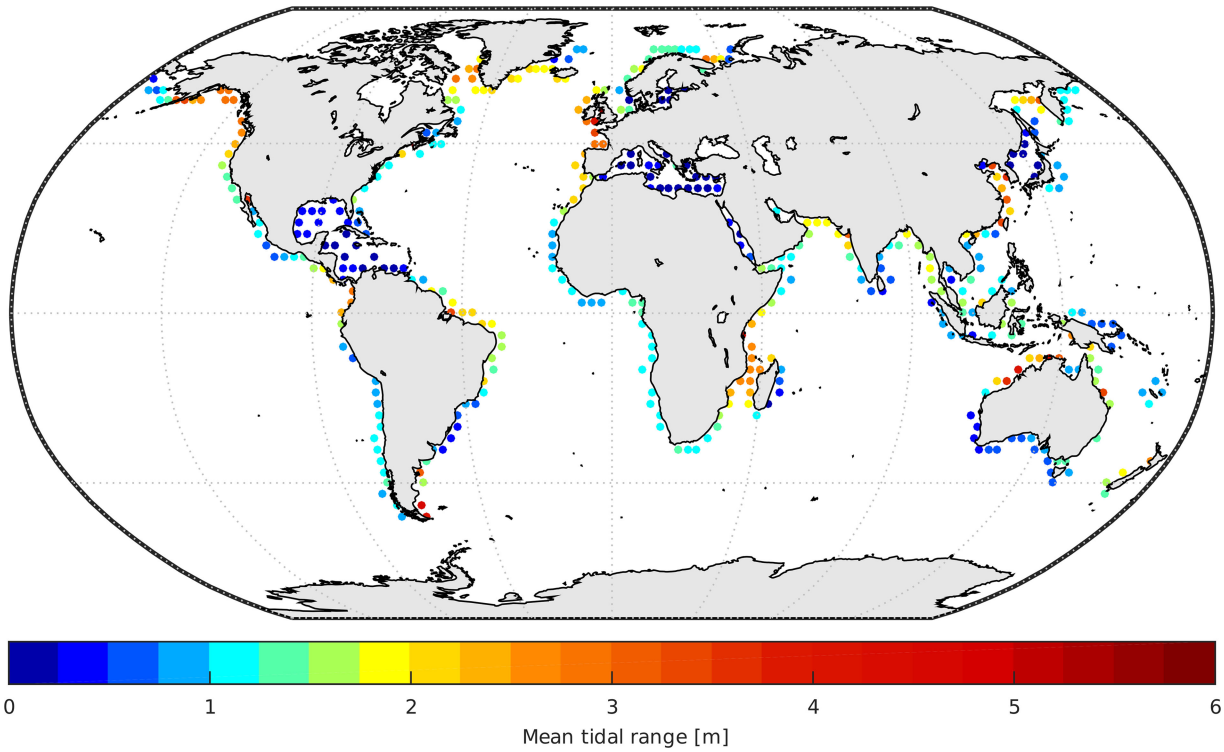

Fig. 3. Mean tidal range at coastal areas. Data acquired from the TMD model.

mately 2.5 m), and the mass of the translator and moving parts (10 tons). Moreover, the Matlab model inputs the hydrodynamic coefficients generated by the software WAMIT, which runs for a cylindrical buoy with 3-m radius and 0.6-m draft [14]. All these parameters and coefficients remain fixed during the simulation process. The WEC model is fed at every iteration with a different (H_s, T_e, H_t) combination, each combination characterizing a coastal point.

The first output of the model is a scatter diagram that contains the generator damping factors γ_i^*, which maximize the WEC

energy conversion P^* at the ith sea state, where $P^* = \gamma^* \dot{x}^2$. Integrating P^* over one year, the annual energy production for the L12 is estimated.

The second output of the model is the estimation of the WEC energy production all over the world, with and without a tidal compensation system, i.e., a device that adjusts the length of the connection line so that the average position of the middle point of the translator always corresponds to the center of the stator. Including the compensation system in the modeling is equal to say $H_t = 0$.

B. Economic Analysis

To optimize γ from a practical point of view, the generator design has to be partially revised and, possibly, an upgrade of the generator itself should be considered. This implies an investment cost that the economic analysis here proposed aims to estimate.

The spinoff company from Uppsala University, Seabased Industry AB, was founded in 2001 to commercialize the wave energy technology and build wave power parks consisting of an array of WEC units. For the purpose of this study, a basic economic assessment is performed for a single unit, the L12. Using data obtained from the manufacturer, we estimate the viable investment cost for a generator upgrade.

Two scenarios are here considered: a suboptimum case, corresponding to a $\gamma_{\rm sub}$ and an optimum case, corresponding to γ^*. The capital expenditures (CAPEX) of the 50-kW WEC were estimated by Seabased to be about 0.25 M€, including operation and maintenance costs. The lifetime of the WEC was assumed to be 24 years in this analysis. Moreover, the net present value (NPV), which provides an indication of how valuable an investment is, is taken into account and it can be used as a reference to know how much it is worth to spend on R&D [15]. The NPV, described in (11), has to be positive for a project to be profitable

$$\text{NPV} = \sum_{i=0}^{N} \frac{C_i}{(1+r)^i} \tag{11}$$

where C_i is the cash flow at year i, and r is the discount rate. Another parameter commonly used to assess the desirability of a project is the internal rate of return (IRR), calculated implicitly as follows:

$$\sum_{i=0}^{N} \frac{C_i}{(1+\text{IRR})^i} = 0. \tag{12}$$

Equation (12) shows that the IRR is the rate at which the investment breaks even. The higher is the IRR, the more attractive is the project.

III. Results

A. WEC Model

As mentioned in Section II, the Matlab model couples the hydrodynamic equation of motion of the buoy with the electromechanical equation of the generator. The buoy position, and consequently the translator position, is influenced by the water level displacement, which is due to the waves and the tide. Fig. 4 shows the water level displacement generated by waves with $H_s = 2$ m, $T_e = 8$ s, and $H_t = 8$ m. This combination

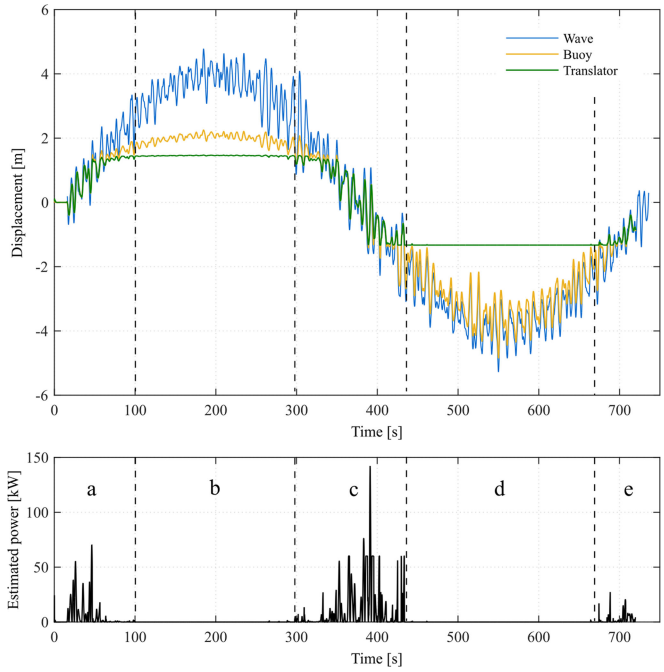

Fig. 4. Simulated behavior of the buoy and the translator positions in semirandom waves superimposed to a sinusoidal tide. The power absorbed by the WEC is illustrated in the lower graph and calculated assuming $\gamma^* = 160$ kNs/m.

was chosen for illustrative purposes. The tidal variability is represented here as having a 12-min period instead of the actual periods of major tidal constituents which are between 12 and 26 h. The optimum choice of modeled tidal period will be discussed later.

Looking at the first section (section "a") of the simulation in Fig. 4, the buoy follows the waves until the water level reaches a certain height; in this section, the translator, driven by the buoy, follows the wave motion. In section "b," the translator pushes continuously against the upper end stop, pulling the buoy underneath the water level; in other words, the translator does not move and the generator does not produce any power. The difference between the buoy and translator displacement curves in section "b" is due to the elasticity of the connection line that is modeled as a spring. In section "c," the tidal level decreases and the translator starts to move again inside the generator, producing electricity. During a low tide, in particular in section "d," the buoy moves freely. Moreover, the draft decreases as the translator is now resting on the lower end stop, hence, the gravity force is balanced by the end-stop force: $F_{gt} = -F_{es}$. Once again, the WEC does not produce any power because the translator does not move.

The behavior of the translator position is influenced not only by the buoy position but also by the damping factor. This means that the energy conversion is affected by the instantaneous water level elevation and by the choice of γ. To find the most suitable γ for a certain wave climate, the simulation has been repeated for different values of the damping factor and in the absence of tides. The result of plotting the estimated annual energy production as a function of the damping factor gives asymmetric convex curves. The curves in Fig. 5 show a peak which corresponds to γ^* for a particular combination of H_s and T_e, and for different

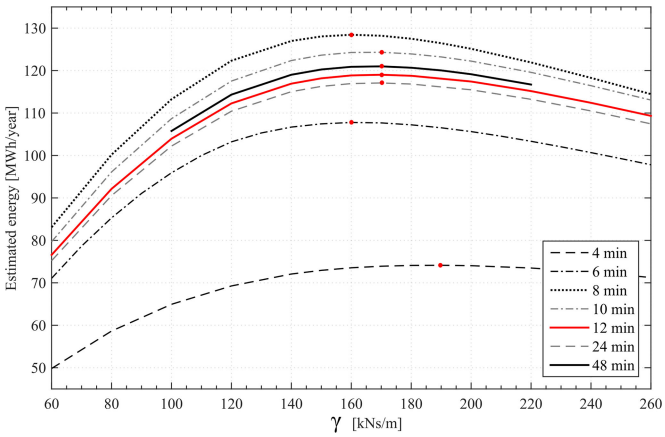

Fig. 5. Annual energy production of one unit wave energy converter as a function of the generator damping factor and simulation time. The wave climate is characterized by $H_s = 2$ m and $T_e = 8$ s. The red dots show γ_i^*.

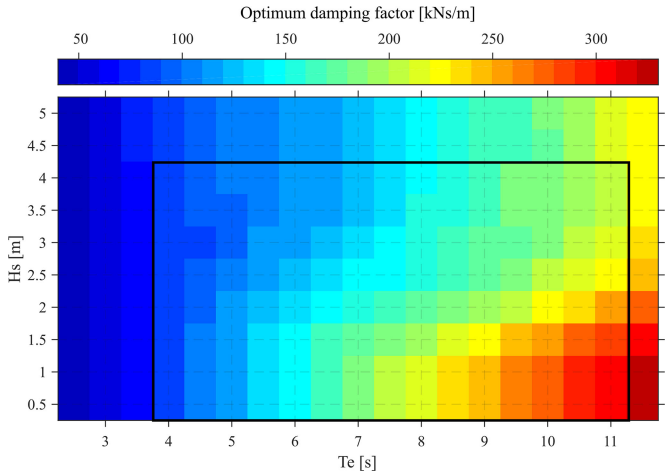

Fig. 6. Scatter diagram indicating the damping factors which maximize the WEC energy output for different wave climates. The values inside the black rectangle are obtained with simulation using an effective tidal period of 12 min, while the other values use 6-min effective periods.

simulation times (i.e., effective tidal periods). Knowing that $P = \gamma \dot{x}^2$, the curves of Fig. 5 would show a limit of the energy function which tends to zero for $\gamma \to 0$. As the damping factor increases, the energy increases until it reaches a peak. After that, the motion of the translator is so damped by γ that its speed decreases until it reaches zero again for $\gamma \to \infty$. Note that the simulations are always run over one complete tidal period, as shown in Fig. 4. The selected periods range from 4 to 48 min. The choice of such short tidal periods is due to the need to speed up the simulations, because of their high computational cost. Fig. 4 shows the influence of the tidal period on the estimation of both the annual energy absorption and γ^*. The optimum effective period is a compromise between being much longer than a wave period but short enough to be computationally feasible. The short tidal period is, then, scaled to match a tidal period of 12 h, which characterizes a semidiurnal tide. Moreover, two tidal cycles per day will be considered in the calculations of the annual estimated energy.

Once a reasonable simulation time is chosen, the same procedure is repeated for every wave climate, and the scatter diagram in Fig. 6 is obtained. The scatter diagram becomes a new input for the calculation of the annual energy production of the WEC with and without the tidal compensation system for the 407 selected locations around the world. The model compares these two outputs and indicates how much power is lost due the tidal effect on the generator (see Fig. 7).

B. Economic Analysis

The red curve in Fig. 5, characterized by $H_s = 2$ m, $T_e = 8$ s, and a 12-min tidal period, is chosen for the implementation of the economic analysis. As mentioned in Section III-A, the short tidal period is scaled to match a realistic tide. The suboptimum scenario is selected to be $\gamma_{\text{sub}} = 80$ kNs/m, which corresponds to an estimated energy production of 92 MWh/year per unit. This translates to 1840 h of utilization time, corresponding to a degree of utilization (DU) of 21%. The DU accounts for the average annual energy delivered to the electric grid, and the rated power of the WEC, which helps to recognize the potential of a renewable source and its possible technical/economic competitiveness [16]. Taking into account only the CAPEX as in [17], and assuming a feed-in tariff of 200€/MWh, the payback time would be about 15 years. In this first scenario, the NPV is negative even with a low discount rate of 5% (see Table I, Case I).

In the second scenario, where the damping factor is chosen to be $\gamma^* = 170$ kNs/m and the energy production reaches up to 120 MWh/year, the utilization time increases to 2380 h and the DU to 27%. Upgrading the system to 170 kNs/m results in a payback time of 11 years (Case II), if we would not consider any additional cost. Moreover, the NPV turns to be positive, and the IRR to be about 7.6%. However, upgrading the system will require an additional cost related to, among others, the increase of the generator size, e.g., the number and/or size of steel plates and magnets used to build a generator. For this reason, the cost of improving the WEC is calculated by comparing not only the NPVs but also different IRRs, as shown in Table I, from Cases II–VIII.

IV. Discussion

A. WEC Model

The hydrodynamic model coupled with the generator equation is able to estimate the wave power production during one tidal cycle, as illustrated in Fig. 4. Electricity is produced as long as the translator moves within the stator, while the production drops to zero during significant high and low tides. During high tides the buoy is submerged, while during low tides the buoy does not feel the gravity force of the translator due to the slack in the line.

For every wave climate, it is possible to establish the optimum generator damping factor, which maximizes the absorbed power. In Fig. 5, the γ^* for the wave climate characterized by $H_s = 2$ m and $T_e = 8$ s is calculated. Each curve has been obtained by increasing the simulation time from 4 to 48 min. As the simulation time increases, the results in terms of γ^* and estimated energy start to converge. A reasonable period was found to be 12 min: the result for that value is fairly close to 48 min and the computation time is significantly reduced.

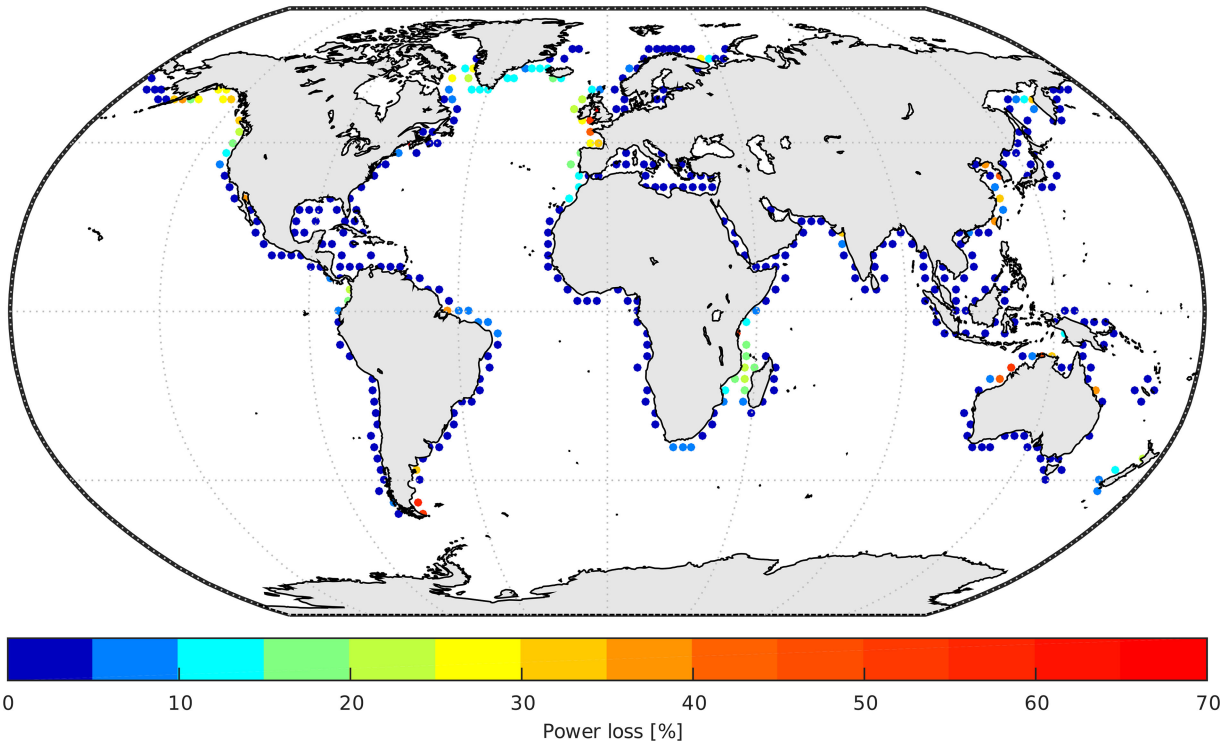

Fig. 7. Percentage of power loss due to the tidal effect on the generator power absorption.

TABLE I
FINANCIAL INDICATORS FOR DIFFERENT SCENARIOS AND GENERATOR UPGRADE COSTS

Scenario γ	*Case no.*	*Upgrade Cost %*	*NPV* ±	*IRR %*	*Payback years*
γ_{sub}	I	0	–	4,8	15
	II	0	+	7.6	11
	III	5	+	7.1	12
	IV	10	+	6.5	12
$\gamma*$	V	15	+	6.0	13
	VI	20	+	5.6	13
	VII	25	+	5.0	14
	VIII	30	–	4.7	14

The scatter diagram in Fig. 6 shows the γ^* for every combination of H_s and T_e based on 12-min simulations within the black rectangle, which includes the most interesting (H_s, T_e). Note that the damping factor increases with the energy period, rather than with the wave height. In other words, the slower is the translator motion, the higher is the damping required to optimize the generator design.

The information contained in Fig. 6 is used as a new input to the model that now aims to calculate the energy lost by the WEC at different locations around the world. This is achieved by comparing the annual energy production of the generator with and without a tidal effect, i.e., with and without a tidal compensation system. The critical areas highlighted in warm colors in Fig. 7 correspond to sites with high tidal range (see Fig. 3). Some of the areas which are subjected to strong tidal effects are located at: the west coast of England and the Bay of Fundy (higher than 60%); the Welsh coast (50%–55%); outside Bretagne, France (40%–45%); the south coast of Argentina (55%–60%); the East China Sea (up to 45%); and the northwest of Australia (up to 55%). The power loss can reach up to 67% and the economic incentive for a tidal compensation system is likely to be high at these locations. Based on the available power from the waves (see Fig. 2) and the power losses due to the tides, the economic benefits of having such a system should be considered.

B. Model Limitations

A brief description of the limitations of the model are here discussed.

First, the buoy and some mechanical parameters of the generator are fixed. This means that the results are true only for L12. If the stroke length of the translator were (subjunctive) increased, the tidal effect could be reduced, but at the same time the costs and the manufacturing challenges would increase. Moreover, the specifications of the end-stops influence the γ^*. If any of the fixed parameters previously discussed are changed in the next version of the Uppsala WECs, the analysis should be updated.

Second, the average wave climate chosen at each location may affect the results of the study. Detailed analyses can be conducted at specific sites to evaluate the goodness of the estimation of the power losses when using the average wave climate rather than the complete $Hs - Te$ scatter diagram.

Third, the hydrodynamic model is based on the linear wave theory, which loses its validity in case of wave runup and for braking waves. However, the theory is assumed to be valid in

section "b" of Fig. 4, because the result in terms of power absorption is not affected.

The values of energy output from the WEC are also influenced by the simulation time of one tidal cycle, as shown in Fig. 5. The choice of using 12 min is reasonable, but more accurate results could be obtained by increasing the time further, albeit with increased computational costs.

Furthermore, the data points in Figs. 2, 3, and 7 are extrapolated from a $3^\circ \times 3^\circ$ grid to give a broad overview on the WEC behavior. Their distances to shore are not always reasonable for the deployment of the WECs. This fact motivates specific case studies to be investigated to give more accurate assessments.

Regarding the modeling of the tide itself, the difference between diurnal, semidiurnal, and mixed tide has been neglected to speed up the simulations. In a specific case study, the time series of the tide could be added as input to the model.

C. Economic Considerations

The analysis considered the upgrade of a WEC from one suboptimum scenario to the optimum scenario.

With reference to Table I, we first show a suboptimum scenario where the damping factor is not optimized to give the maximum absorbed power. Second, the analysis incorporates a technology upgrade that results in the highest estimated energy production (see Fig. 5). In the first scenario, corresponding to Case I, the expected present value of the cash flow is negative. In contrast, the second scenario brings additional value to the investment. With an upgraded system (Cases II–VII), the WEC energy production reaches up to 120 MWh/year, resulting in a DU of 27%, a positive NPV, a higher IRR, and a lower payback period, thus demonstrating the profitability of the project.

For the optimized system to be cost effective, the analysis in Case V suggests that the additional expenditure required to improve the performance of the WEC should be up to 15% of the initial CAPEX, given that the accepted IRR for marine energy projects can be as low as 6% [18]. Table I shows that the payback period in Case V is almost half of the WEC lifetime and gives a sufficiently high IRR, which is still attractive for potential future investors.

V. Conclusion

The paper describes the performance of the present generation Uppsala University WEC, at different locations around the world, i.e., for different combinations of significant wave height, energy period, and tidal range. To carry out this evaluation, a hydromechanic model which analyses the optimum generator damping factor and the WEC power absorption is developed.

The L12 energy conversion has been simulated and the effect of the tides estimated. The optimum generator damping factor is calculated for different wave climates and summarized in a scatter diagram.

An economic assessment is carried out showing the viable additional investment of a generator upgrade. In the specific case analyzed within the paper, an additional cost of up to 15% of the initial cost of the WEC could be viable using an IRR of 6% as a reference. Even though a basic economic assessment is performed, the present study underscores the potential benefits of upgrading the design, if necessary, and therefore the importance of investigating the damping forces when dimensioning the generator for a specific location.

The power loss of the WEC due to the tidal effect is evaluated for near-coastal sites all around the world and critical areas are highlighted for future investigation. The model described within this paper can be used to describe the behavior of the WEC at specific locations in more detail and with more accurate results.

Moreover, the energy loss per meter of tide can be estimated and the findings will influence the mechanical design of the tidal compensation system or the size of the translator stroke length. In the future, this study could be extended from the analysis of a single unit to a farm of WECs.

Acknowledgment

The authors would like to thank J. Engström for running the WAMIT simulation tool, and I. Dolguntseva and B. Ekergård for their comments on the manuscript.

References

[1] M. Leijon *et al.*, "Wave energy from the North Sea: Experiences from the Lysekil Research Site," *Surv. Geophys.*, vol. 29, no. 3, pp. 221–240, 2008.

[2] H. Polinder, M. A. Mueller, M. Scuotto, and M. Goden de Sousa Prado, "Linear generator systems for wave energy conversion," in *Proc. 7th Eur. Wave Tidal Energy Conf.*, Porto, Portugal, Sep. 2007.

[3] E. Lejerskog, C. Boström, L. Hai, R. Waters, and M. Leijon, "Experimental results on power absorption from a wave energy converter at the Lysekil wave energy research site," *Renew. Energy*, vol. 77, pp. 9–14, 2015, DOI: 10.1016/j.renene.2014.11.050.

[4] M. Stålberg, R. Waters, O. Danielsson, and M. Leijon, "Influence of generator damping on peak power and variance of power for a direct drive wave energy converter," *J. Offshore Mech. Arct. Eng.*, vol. 130 no. 3, 2008, DOI: 10.1115/1.2905032.

[5] S. Tyberg *et al.*, "Wave buoy and translator motions—Onsite measurements and simulations," *IEEE J. Ocean. Eng.*, vol. 36 no. 3, pp. 377–385, 2011.

[6] V. Castellucci, J. Abrahamsson, O. Svensson, and R. Waters, "Algorithm for the calculation of the translator position in permanent magnet linear generators," *J. Renew. Sustain. Energy*, vol. 6, 2014, DOI: /10.1063/1.4900553.

[7] M. Eriksson, R. Waters, O. Svensson, J. Isberg, and M. Leijon, "Wave power absorption: Experiments in open sea and simulation," *J. Appl. Phys.*, vol. 102, 2007, 084910, http://dx.doi.org/10.1063/1.2801002

[8] L. Hai *et al.*, "Force in the connection line for a wave energy converter: simulation and experimental setup," in *Proc. 3rd Int. Conf. Ocean Offshore Arctic Eng.*, 2014, DOI: 10.1115/OMAE2014-23147.

[9] S. K. Chakrabarti "Hydrodynamics of offshore structure," *Computational Mechanics*. Southampton, U.K.: WIT Press, 1987, ch. 4.

[10] ERA-Interim reanalysis datasets, http://apps.ecmwf.int/datasets/data/interim-full-daily

[11] S. Barstow, G. Mϕrk, L. Lϕnseth, and J. P. Mathisen, "Worldwaves wave energy resource assessments from the deep ocean to the coast," in *Proc. 8th Eur. Wave Tidal Energy Conf.*, Uppsala, Sweden, 2009.

[12] S. H. Salter, "Wave power," *Nature*, vol. 249, pp. 720–724, 1974.

[13] G. D. Egbert and S. Y. Erofeeva, "Efficient inverse modeling of barotropic ocean tides," *J. Atmos. Ocean. Technol.*, vol. 19, no. 2, pp. 183–204, 2002.

[14] M. Terzi, "Compensation system for high range mean sea level variations designed for wave power plants. Mechanical design and hydrodynamic modelling," M.S. thesis, Dept. Eng. Sci., Uppsala Univ., Uppsala, Sweden, 2015, http://hdl.handle.net/10589/107436

[15] M. West *et al.*, "Alternative energy systems: Electrical integration and utilisation," Oxford, U.K.: Permanon, 1984, pp. 139–162.

[16] A. Skoglund, M. Leijon, A. Rehn, M. Lindahl, and R. Waters, "On the physics of power, energy and economics of renewable electric energy sources—Part II," *Renew. Energy*, 2010, DOI: 10.1016/j.renene.2009.08.031.

[17] J. Cordonnier, F. Gorintin, A. De Cagny, A. H. Clment, and A. Babarit, "SEAREV: Case study of the development of a wave energy converter," *Renew. Energy*, vol. 80, pp. 40–52, 2015, doi:10.1016/j.renene.2015.01.061.
[18] G. Allan, M. Gilmartin, P. McGregor, and K. Swales, "Levelised costs of wave and tidal energy in the UK: Cost competitiveness and the importance of banded renewables obligation certificates," *Energy Policy* vol. 39, pp. 23–39, 2011.

Valeria Castellucci received the M.S. degree in environmental and land planning engineering from Politecnico di Milano, Milan, Italy, in 2011. She is currently working toward the Ph.D. degree at the Division of Electricity, Uppsala University, Uppsala, Sweden, with special focus on the tidal compensation system for wave energy converters in the frame of the Lysekil Research Project.

Jessica García-Terán received the M.S. degree in sustainable development from Uppsala University, Uppsala, Sweden, where she is currently working toward the Ph.D. degree at the Department of Industrial Engineering and Management.

She has been working with renewable energy technologies, particularly wave and marine current power. Currently, her research relates to the commercialization of these technologies and innovation management for complex systems.

Mikael Eriksson received the M.Sc. degree in engineering physics and the Ph.D. degree in electricity with emphasis on wave power from Uppsala University, Uppsala, Sweden, in 2002 and 2007, respectively.

During 2007–2015, he worked at Seabased AB, a Swedish wave power company. He is currently a Researcher at the Division of Electricity, Uppsala University. His main research interests are wave power and hydromechanical renewable energy conversion.

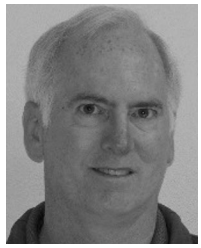

Laurence Padman received the B.S. degree in marine sciences and the Ph.D. degree in oceanography from the University of Sydney, Sydney, N.S.W., Australia, in 1981 and 1987, respectively.

After graduating, he worked at Oregon State University, Corvallis, OR, USA, as a Postdoctoral Associate and Research Professor specializing in polar oceanography. In 1997, he joined the Seattle-based nonprofit company, Earth & Space Research, Corvallis, OR, USA, as a Senior Scientist and is now Vice-President.

Dr. Padman is currently a Senior Editor for *Antarctic Science*, and recently received the American Meteorological Society (AMS) Editor's Award for reviewing for the *Journal of Physical Oceanography*. He is a member of the AMS, the American Geophysical Union, the Oceanography Society, and the International Glaciological Society.

Rafael Waters received the Ph.D. degree from Uppsala University, Uppsala, Sweden, in 2008, receiving Bjurzon's premium for excellent Ph.D. dissertation by the vice chancellor of the university.

He is an Associate Professor specialized in renewable electricity production from ocean waves. He works at the Division for Electricity, Uppsala University. He was Head of the Power Plant Design Department, Seabased Industry AB (2009–2012). Currently, he is a project leader for the Lysekil Research Project.

Dr. Waters received the Gran Gustavsson prize for younger scientists.